Proceedings World Geothermal Congress 2020+1
Reykjavik, Iceland, April - October 2021

Time-lapse Micro-gravity Monitoring of the Theistareykir and Krafla Geothermal Reservoirs (Iceland)

Nolwenn Portier[1], Jacques Hinderer[1], Vincent Drouin[2,4], Freysteinn Sigmundsson[2], Florian Schäfer[3], Philippe Jousset[3], Kemâl Erbas[3], Andreas Güntner[3], Ingvar Magnússon[4], Gylfi Páll Hersir[4], Kristján Ágústsson[4], Elske De Zeeuw van Dalfsen[5], Ásgrímur Guðmundsson[6], Egill Juliusson[6], Jean-Daniel Bernard[1]

1. IPGS (Institut de Physique du Globe de Strasbourg), Université de Strasbourg/CNRS, France 2. University of Iceland, Reykjavik, Iceland 3. Helmholtz Centre Potsdam GFZ German Research Centre for Geosciences, Potsdam, Germany 4. ÍSOR Iceland GeoSurvey, Reykjavik, Iceland 5. KNMI (Koninklijk Nederlands Meteorologisch Instituut), De Bilt, Netherlands 6. Landsvirkjun, National Energy Company, Iceland

nolwenn.portier@unistra.fr

Keywords: Theistareykir, Krafla, geothermal energy, monitoring, time-lapse micro-gravity

ABSTRACT

We use the micro-gravity time-lapse method to monitor the subsurface mass changes induced by the geothermal energy exploitation at the Krafla and Theistareykir geothermal fields. The two sites are located on the path of the Mid-Atlantic ridge in northeastern Iceland. The Theistareykir plant produces 90 MWe since 2017 thanks to a geothermal fluid of around 300°C extracted from 13 wells at 2 to 2.5km depth. The Krafla geothermal operation began in 1977 and reached a power production capacity of 60 MWe in 1997. We study both the short and long-term impact of the geothermal reservoir production.

We carried out time-lapse relative micro-gravity surveys in summer 2017 and 2018 using a Scintrex CG5 gravimeter at both sites. The stations were chosen according to previous gravity campaigns by ISOR (Magnússon, 2012, 2014, 2016) and De Zeeuw-van Dalfsen et al. (2006). After tidal and instrumental drift corrections, we calculated the double differences in gravity, which show the gravity variation at each measurement point compared to a reference time and station. The stability of the reference station was investigated by repeated absolute measurements with the Micro-g solutions FG5#206 ballistic absolute gravimeter. Since December 2017, continuous gravity measurements were performed by GFZ Potsdam, using three superconducting gravimeters and one gPhone, to obtain high-resolution time series of gravity changes at the geothermal fields (see WGC2020 paper of Erbas et al., n°13124). To determine the mass redistribution, gravity data are corrected for the ground vertical motion by using GPS measurements performed by the University of Iceland (see WGC2020 papers of Drouin et al., n°13143 and Sigmundsson et al., n°13174).

Considering the gravity variations corrected for the vertical displacements, we observe a gravity increase close to the injection area at the Krafla site. On the contrary, we notice a general decrease in gravity at the Theistareykir geothermal area with a maximum value in vicinity to the production zone, between the 2017 and 2018 surveys.

1. INTRODUCTION

Iceland results from an intensive volcanic activity induced by the interaction of a hot spot due to a deep-sealed mantle plume (Wolfe et al., 1997) and the Mid-Atlantic ridge. It is on the boundary between the North American tectonic plate and the Eurasian one which drift apart with a velocity of around 2 $cm.y^{-1}$. This tectonically active place characterized by volcanoes, hot spring and fumaroles, is suitable to harness geothermal energy. In 2017, the cumulative capacity of the geothermal plants was 710 MWe (Orkustofnun, 2017) which is around 25% of the produced electricity in the country. However, the sustainability of a power plant producing this renewable energy depends on the balance between heat and fluid outflow associated to the production and heat and fluid inflow into the reservoir (Axelsson, 2011). The recharge fluid comes from the re-injection of the produced geothermal water or/and from the surrounding area. Moreover, injection and production flow rates have to be adapted so as not to cool the geothermal system: the recharge fluid should have time to be warmed up by the natural earth heat flow. The time-lapse micro-gravity method highlights sub-surface mass redistribution and, hence, can help estimating recharge of the geothermal reservoir. For instance, after a temporary shutdown for maintenance of the Ogiri Geothermal Field (Kirishima volcano, Japan), Nishijima et al. (2016) measured a gravity decrease of about 20 µGal (1 µGal = 10^{-8} $m.s^{-2}$) in the reinjection area and a gravity increase up to 30 µGal in the production area. In the same way, Portier et al. (2018), following a feasibility study by Hinderer et al. (2015), performed a time-lapse micro-gravity survey at the Soultz-sous-Forêts enhanced geothermal system (Alsace, France). They showed a differential signal consistent with the injection and production areas. Here, we apply this method to monitor two geothermal fields in the Northern Volcanic Zone (NVZ) of Iceland, Krafla (60 MWe) and Theistareykir (90 MWe).

2. METHODOLOGY

2.1 The hybrid micro-gravity

The hybrid micro-gravity method was first introduced by Okubo et al. (2002). This method combines three types of gravimeters (Hinderer et al., 2016):

- A permanent relative gravimeter like a superconducting gravimeter which measures continuously the gravity variation at a reference station;
- An absolute gravimeter to calibrate and correct for the instrumental drift of the permanent gravimeter;
- A spring relative gravimeter to investigate the gravity changes at several stations with respect to a reference station.

We performed time-lapse relative and absolute gravity measurements at the Theistareykir and Krafla geothermal fields in summer 2017 and 2018, with a Scintrex CG5#41317 and Micro-g Solutions Inc. FG5#206 gravimeters, respectively. Furthermore, in the framework of MicroGraviMoTis project, GFZ Potsdam deployed three superconducting gravimeters (iGrav32, iGrav15 and iGrav6) and one gPhone (#128) at the Theistareykir geothermal area in December 2017 (see WGC2020 paper of Erbas et al., n°13124).

2.2 The data processing

The instrumental drift of the time-lapse relative gravity measurement is removed using the Python PyGrav software (Hector and Hinderer, 2016) before the gravity double differences $Dg_{x-x_0}^{t-t_0}$ are calculated (see equation 1). They show the gravity variation at a time t and at a station x with respect to a reference time t_0 and a reference station x_0. g_x is the gravity value measured at the station x.

$$Dg_{x-x_0}^{t-t_0} = (g_x - g_{x_0})_t - (g_x - g_{x_0})_{t_0} \quad (1)$$

The error is obtained by calculating the square root of the sum of the variances of the four gravity terms g in equation (1). It is correlated to the quality of the drift correction. To highlight the sub-surface mass changes, the gravity double differences must also be corrected for the gravity changes due to vertical displacement (Hunt et al., 2002). We measured the gravity free-air gradient (FAG) at the absolute gravity stations (see Fig. 4 and 8) i.e. three and one sites at the Theistareykir and Krafla fields, respectively. We find that vertical ground movements induce a change of 3.2 +/- 0.1 µGal.cm^{-1} and 2.959 +/- 0.004 µGal.cm^{-1} at the Theistreykir and Krafla area, respectively. To apply this vertical displacement correction, we use GPS measurements performed by the University of Iceland (see WGC2020 papers of Drouin et al., n°13143 and Sigmundsson et al., n°13174).

3. THE THEISTAREYKIR GEOTHERMAL FIELD

3.1 Geological and geothermal framework

The Theistareykir geothermal field is located at the intersection between the Northern Rift Zone (NRZ) and the Tjörnes Fracture Zone (TFZ) in northeast Iceland. Its bedrock is constituted by both sub-glacial eruption products (hyaloclastites, typically formed of pillow basalts, breccias and tuffs) and recent basaltic lava flows (younger than 10,000 years) (see Fig. 1).

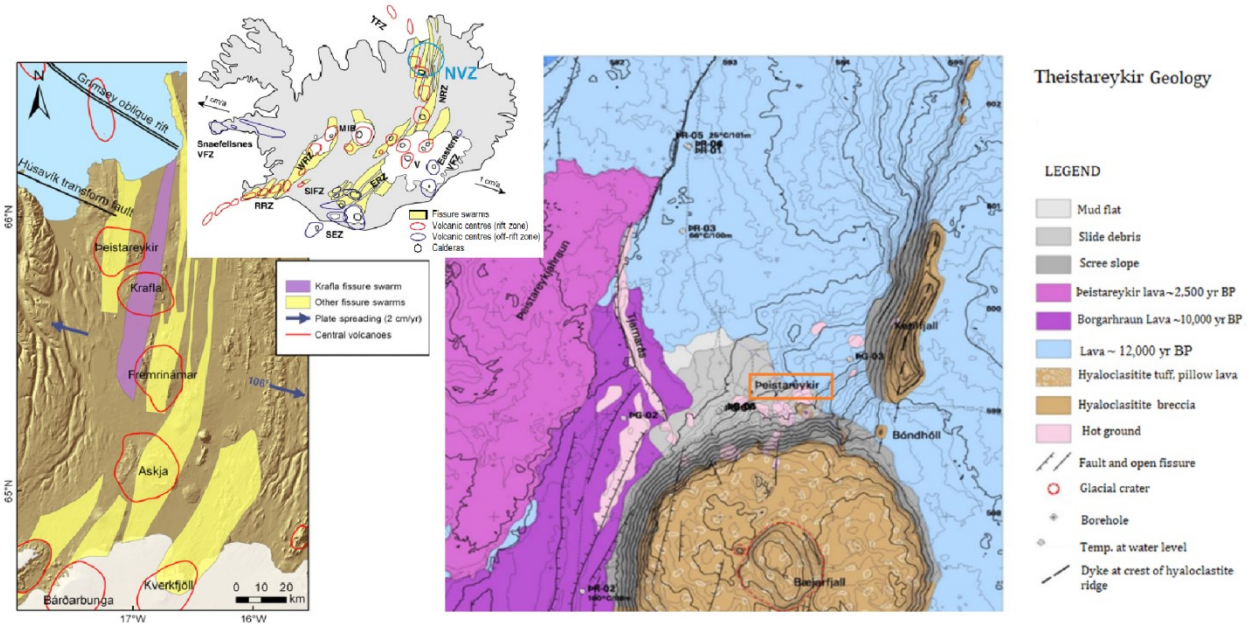

Figure 1: Location (from Mkangala, 2017 and Hjartardóttir et al., 2012) and geological map (from Saemundsson, 2007) of the Theistareykir geothermal field.

Surface exploration of the 11km^2 geothermal area at Theistareykir started in the 1970s. Based on gas geothermometers studies of 34 fumaroles, Armannsson et al. (1986) identified three promising areas for exploitation, the D, C, A areas (see Fig. 2). Hence, following the drilling of four shallow wells to characterize the groundwater table, the first exploration borehole was drilled in 2002 (Armannsson, 2008). By 2008, five additional boreholes were created, allowing Gudmundsson et al. (2008) to refine a conceptual model of the Theistareykir geothermal system (see Fig. 2). According to this work, a powerful up-flow would maintain a 300°C vapor between 1.5 km and 2 km. Furthermore, the migration of the primary steam and its condensation would supply shallower cavities with a 250-280°C liquid phase except on the east part of the geothermal field. There, the primary steam would be cooled to 200°C in open fractures. Gudmundsson et al. (2008) estimated the potential of the geothermal system to be 104MWe for 100 years of production.

Consequently, following an environmental impact assessment (Mannvit, 2015), the construction of the plant started in April 2015. The first phase began to produce 45 MWe in Autumn 2017. The second phase started in Spring 2018 and reached a total production of 90 MWe. The power plant currently uses 13 production wells, at 2 to 2.5 km depth which extract hot geothermal fluid.

Production temperatures range between 280 and 330°C. The condensed steam is re-injected by 2 co-located wells at 450m depth, with a flow rate of around 200L.s^{-1}.

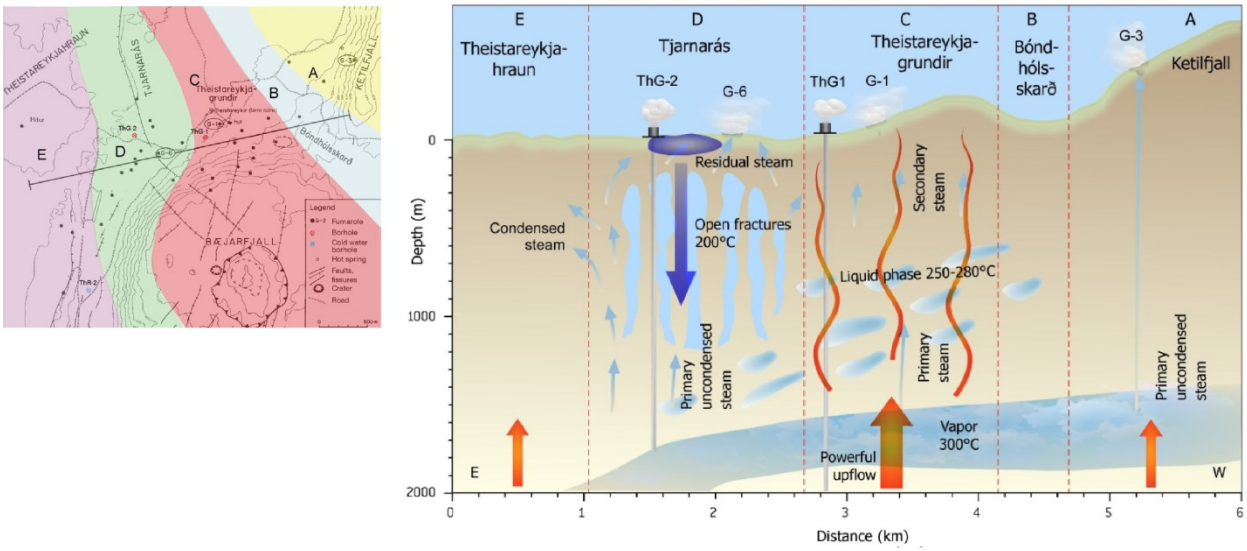

Figure 2: A conceptual model of the Theistareykir geothermal system (from Gudmundsson et al., 2008 and Armansson et al, 1986)

To improve the understanding of the geothermal reservoir, several geophysical surveys have been conducted. For instance, transient electromagnetic (TEM) and magnetotelluric (MT) measurements were performed in 2004-2006 and 2009-2011, respectively. The results show that the resistivity structure of the Theistareykir field can be divided in four zones, from top to bottom (Árnason et al., 2008, Karlsdóttir et al., 2012):

- A resistive area characterized by unaltered rock formations (zone 1);
- The smectite-zeolite zone forming a low resistivity cap (zone 2);
- The mixed layered clay zone where resistive chlorite replaces smectite, and zeolite disappears (zone 3);
- The resistive chlorite-epidote area (zone 4).

Kahwa (2012) explains that the low resistivity cap (zone 2) reaches the surface in the Theistareykir production area (see Fig. 3). It implies that the south-north sub-surface fluid flow circumvents this zone.

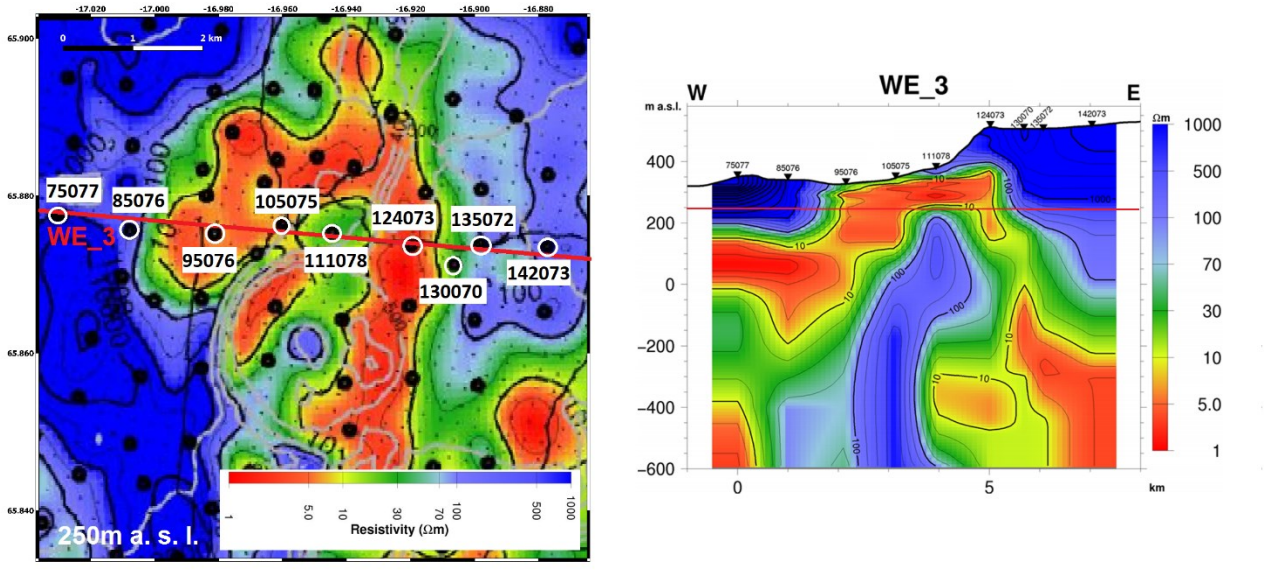

Figure 3: Figure to the left: Map of the top of the low resistivity cap (250m a.s.l.) at Theistareykir based on 3D inversion of MT data (from Karlsdóttir et al., 2012). Figure to the right: WE_3 Resistivity profile obtained by inverting TDEM measurements is also shown (from Kahwa, 2012)

Gravity measurements were performed in 1981-1983 (Gislason et al., 1984). They highlighted a low gravity structure at the intersection between the Theistareykir fissure swarm and the Husavik fracture zone. ISOR (Magnússon, 2016) repeated the gravity measurements in 2011 and 2015. We conducted time-lapse micro-gravity measurements at the same gravity stations before and after the beginning of the electricity production, in summer 2017 and 2018.

3.2 The time-lapse micro-gravity network

We measured a network of 27 stations (see Fig. 4 and Table 1) at the Theistareykir geothermal field.

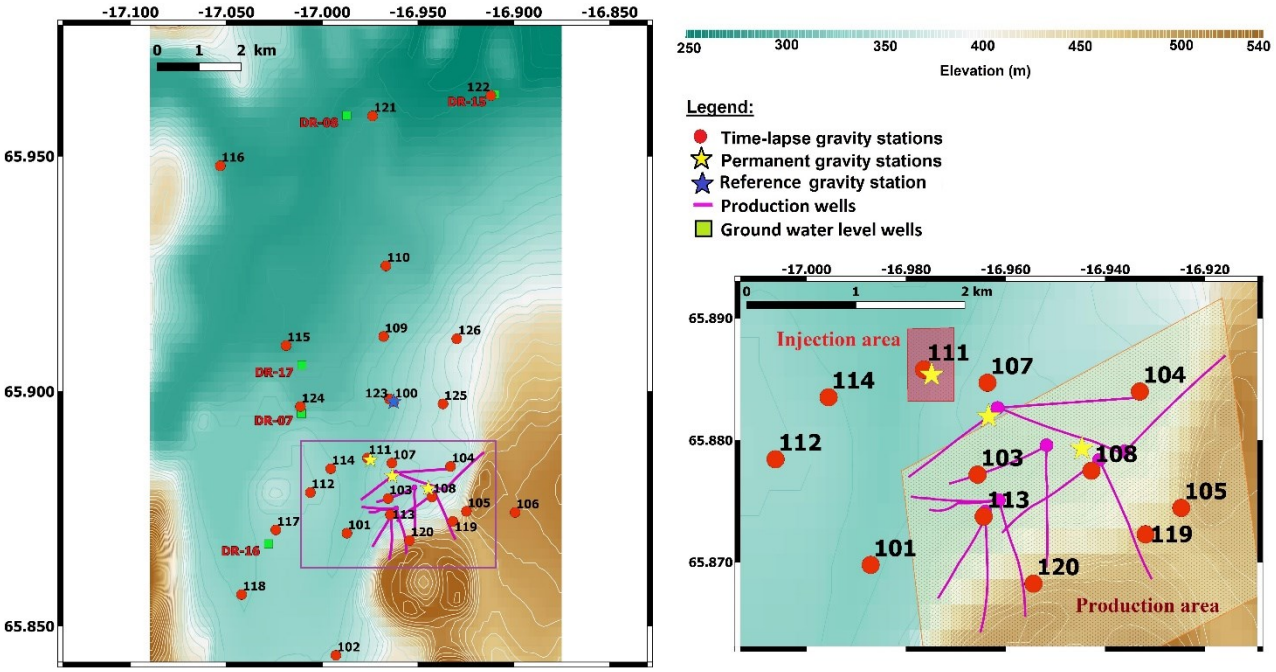

Figure 4: The gravity network of the Theistareykir geothermal field. The figure to the right is an enlargement of the figure to the left (the purple rectangle). The background topography is from GMTED 2010 with 7.5 arc seconds resolution (www.usgs.gov). The reference station of the time-lapse relative measurements is shown by a blue star. It was measured with the absolute gravimeter, which was also used to measure the permanent gravity stations (yellow stars). We also represent the ground water level wells (green squares).

Table 1: Coordinates of the gravity stations at the Theistareykir geothermal field.

Stations	Lat.	Lon.
100	65.89776°N	-16.96273°E
101	65.86977°N	-16.98710°E
102	65.84372°N	-16.99283°E
103	65.87717°N	-16.96562°E
104	65.88398°N	-16.93304°E
105	65.87444°N	-16.92473°E
106	65.87420°N	-16.89934°E
107	65.88470°N	-16.96364°E
108	65.87749°N	-16.94277°E
109	65.91166°N	-16.96795°E
110	65.92667°N	-16.96677°E
111	65.88578°N	-16.97639°E
112	65.87843°N	-17.00620°E
113	65.87373°N	-16.96441°E

Stations	Lat.	Lon.
114	65.88351°N	-16.99554°E
115	65.90973°N	-17.01884°E
116	65.94793°N	-17.05316°E
117	65.87048°N	-17.02420°E
118	65.85670°N	-17.04206°E
119	65.87228°N	-16.93189°E
120	65.86823°N	-16.95439°E
121	65.95851°N	-16.97372°E
122	65.96284°N	-16.91195°E
123	65.89834°N	-16.96486°E
124	65.89674°N	-17.01134°E
125	65.89731°N	-16.93696°E
126	65.91116°N	-16.92977°E

3.3 The gravity double differences

The gravity double differences recorded in 2018 with respect to 2017 are shown in Figure 5. They are corrected for the gravity changes due to vertical displacement. The vertical ground motion is deduced from GPS measurements and from InSAR analysis that the University of Iceland is currently performing. Drouin et al. describe the deformation study of the Theistareykir geothermal field in WGC2020 paper n°13143. We only present the gravity stations co-located with a GPS site.

We notice a decrease of -2.0 +/- 1.4 µGal at the reference station, measured by the absolute gravimeter. The gravity double differences are corrected for this variation. Consequently, a general gravity decrease is observed in the studied area with maximum values of -23 +/- 11 µGal at the station 108 and -21 +/- 5 µGal at the station 124.

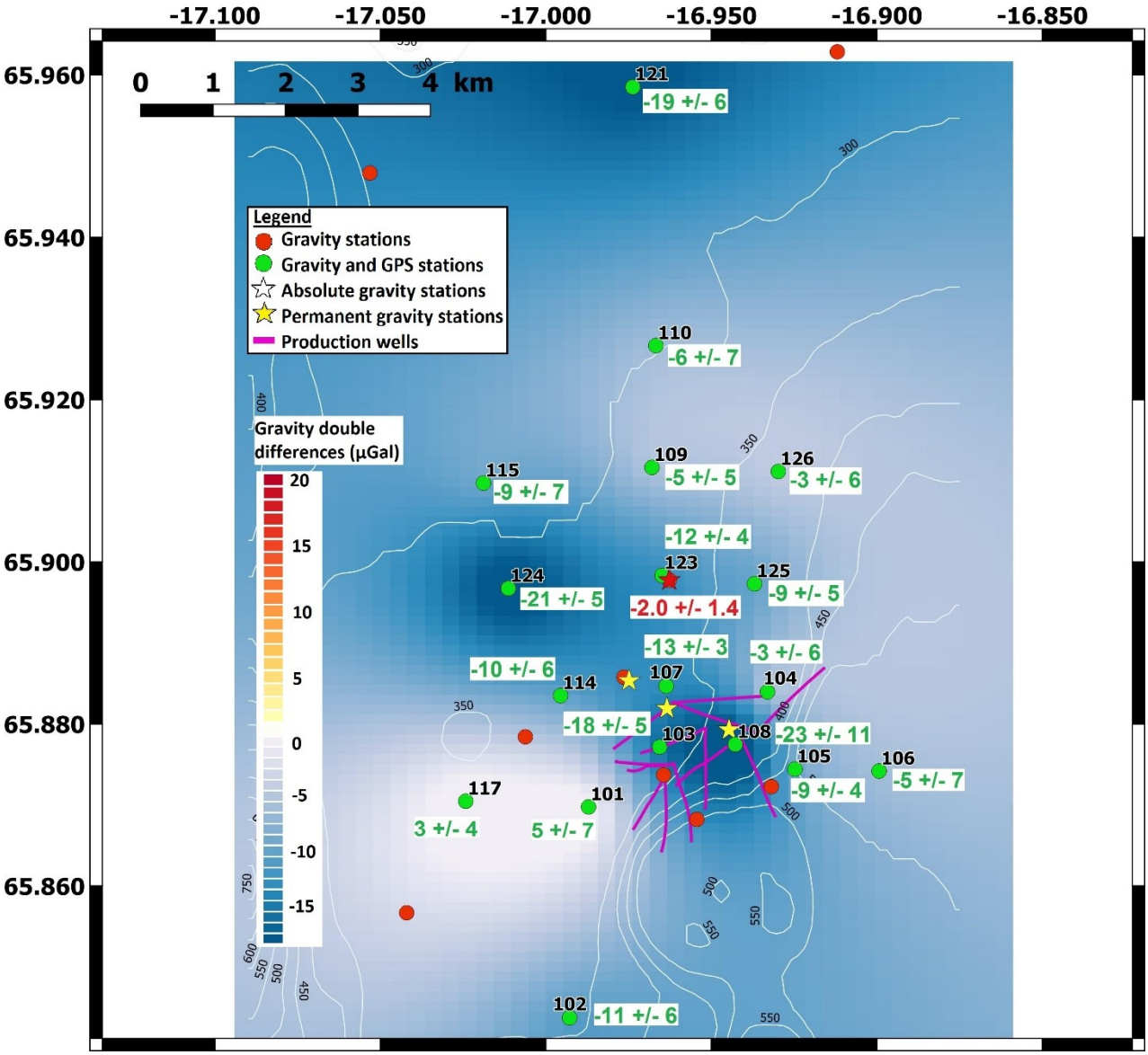

Figure 5: Map of the gravity double differences corrected for the vertical displacement (-3 µGal.cm^{-1}) and the gravity variation of the reference station (red star) measured at the Theistareykir geothermal field in 2018 with respect to 2017. The gravity data have been interpolated using a kriging method. We distinguish the time-lapse relative stations co-located with GPS sites (green circle) from those which are not (red circle). Black numbers close to the station dots are station number. The production wells are depicted in purple. Elevation isolines (m) are white thin lines. Absolute measurements have been performed at all the stations represented by stars, especially at the permanent gravity stations (yellow stars). The relative and absolute gravity change values are written in green and red, respectively.

3.4 Modelling gravity changes

As a first attempt, we explain the measured gravity double differences using a simplistic model based on two Mogi spheres (Mogi, 1958) (see Fig. 6). One Mogi sphere represents the total produced mass estimated equal to around 6.5 MT (Egilson, 2019) between 2017 and 2018. It is 1.6 km depth. The second Mogi sphere is located at 1.8 km depth below the station 124 and represents a mass change of -9 MT. We do not yet understand its origin. These two mass changes induce the calculated gravity double difference $Dg_{cal}^{2018-2017}$ (see equation (2)) that we compare to the measured gravity change (see Fig. 6).

$$Dg_{cal}^{2018-2017} = G * \sum_i \frac{M_i * z_i}{\sqrt{d_i^2 + z_i^2}^3} \quad (2)$$

G is the gravitational constant (6.67×10^{-11} m^3 kg^{-1} s^{-2}). M_i and z_i are the mass variation and the depth of the source i. d_i is the distance to the projection on the surface of the source i.

We do not explain the value measured at the station 104 of -3 +/- 6 µGal. Considering the error, a difference of 1 µGal is observed with the modelled gravity double differences of 10 µGal. In the same way, we note that the increase in gravity double differences at the stations 101 and 117 is not explained by our model. However, in our analysis we do not yet consider the injected geothermal fluid estimated equal to 2.3 MT considering a 200 L/s flow rate. One possibility is that the injected fluid is drained through SN faults (see Fig. 6) in the SW part of the study area (below the stations 117 and 101 (see Fig. 2)).

We do not understand what would be the origin of the mass change near the station 124. It seems that Magnússon (2016) observed it between 2011 and 2015 with an opposite sign i.e. a gravity increase. However, Egilson (2019) noticed that, following the beginning of the geothermal fluid re-injection, the ground water level is increasing of around 1 m at the well DG-07 (see Fig. 7) close to the station 124 between the two gravity campaigns (2017-2018). This effect should result in an increase in gravity that we do not measure. It would also suggest that the re-injection water goes to the northeast area and would stay in sub-surface instead of going deeper to the SW part as mentioned above. These assumptions will be tested with new time-lapse micro-gravity measurements in summer 2019.

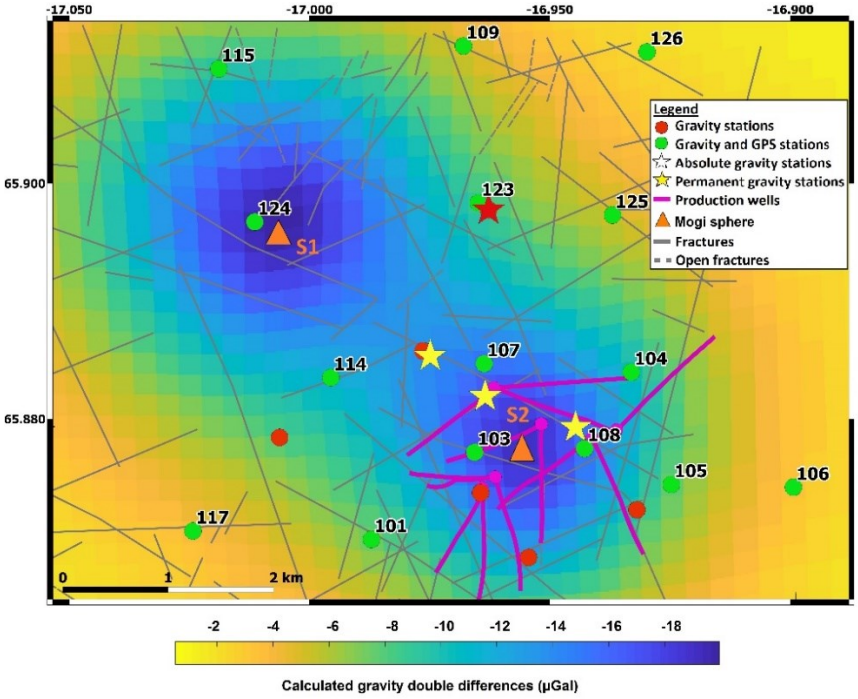

Gravity station	Measured gravity double differences (µGal)	Calculated gravity double differences (µGal)
101	*5 +/- 7*	*-7*
103	-18 +/- 5	-17
104	*-3 +/- 6*	*-10*
105	-9 +/- 4	-8
106	-5 +/- 7	-3
107	-13 +/- 3	-15
108	-23 +/- 11	-15
109	-5 +/- 5	-5
114	-10 +/- 6	-12
115	-9 +/- 7	-9
117	*3 +/- 4*	*-4*
123	-12 +/- 4	-9
124	-21 +/- 5	-19
125	-9 +/- 5	-5
126	-3 +/- 6	-2

Figure 6: Map of the modeled gravity double differences in µGal at the Theistareykir geothermal field (right). Two Mogi spheres (S1 and S2) are considered. S1 is located at 1.8 km depth and represents a mass change of -9 MT. S2 is located at 1.6 km depth and represents a mass change of -6.5 MT (Geothermal fluid production). We also represent the most significant fractures in the area (grey lines) (from Khodayar and Björnsson, 2013). The measured and calculated values are compared in the table (right). The gravity double differences of three stations (101, 104 and 117) are the only ones not explained by this model (written in italic).

4. THE KRAFLA GEOTHERMAL FIELD

4.1 Geological and geothermal framework

The Krafla volcanic system is located in the Northern Volcanic zone (NVZ) (see Fig. 1). It is characterized by a 9x7 km² caldera formed about 110,000 years ago which intersects a N-S trending fissure swarm, with a length of 100 km and a width of 5-8 km (Hjartardóttir et al., 2012). According to the gravity Bouguer anomaly, this caldera, filled with volcanic materials, includes a second buried caldera probably formed after the area was covered with ice 80,000 years ago (Árnason et al., 2007) (see Fig. 7). During the Holocene, we can identify two periods of intensive eruptive activities: 1) >3000 years ago and 2) <3000 years ago. The first period was characterized by volcanic eruptions concentrated in the east part of the NVZ until spreading shifted to the western part of the caldera ("Hvannstóð-period") and ended when activity came back to the east part. The second period, which is still ongoing today, was characterised by two rifting episodes: the 1724-1729 Mývatn Fires and the 1975-1984 Krafla Fires. The explosive crater Viti formed during the Mývatn Fires and is the youngest eruptive formation within the Krafla system (Saedmundsson, 1991). At the same time as this first rifting event (Mývatn Fires), Einarsson (1978) studied the S-wave attenuation and suggested the presence of a magma chamber at 3-8km depth. Magnetotelluric (MT) soundings performed in 2004-2006 highlight three deep conductors interpreted as chimneys in the inner caldera (Árnason et al., 2007) (see Fig 7). These studies also show a ESE-WNW low gravity anomaly and high resistivity lineament (graben) which could be due to transform tectonics.

The Krafla volcanic system counts two main geothermal fields: the Bjarnarflag (Námafjall high temperature area) and the Krafla geothermal fields. The first one is dedicated to the production of hot water for the town of Reykjahlið and for a geothermal pool. Since 1969, a production of 3 MW is achieved using 1500-2500 kT.y^{-1} (Drouin et al., 2017). The construction of the Krafla field was initiated in 1975, after having drilled two exploration wells in 1974. The geothermal operation started in 1977 and reached a

power production capacity of 60 MWe in 1997. Around 9,000 kT of water and steam have been extracted each year since 2000 (Drouin et al., 2017). In 1999, re-injection was initiated, reaching a mass extraction of 4,000 kT in 2014. The Krafla geothermal field can be divided in at least three different reservoirs (Langella et al., 2017) (see Fig. 8):

- Suðurhlíðar : a two phase system about 2 km to shallow depths;
- Leirbotnar: a deep two phase zone below 1-1.5 km overlaid by a 200-1100m depth liquid saturated zone;
- Hvíthólar: a two phase area overlaid by a 170-190°C water-saturated zone at 600m depth.

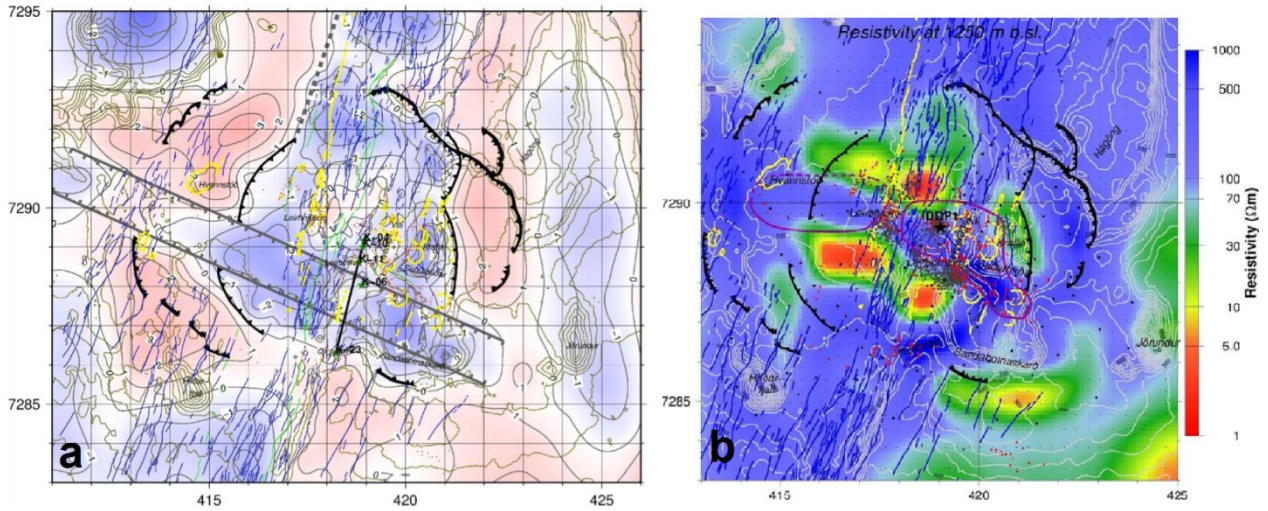

Figure 7: Maps of the Krafla volcano. The hedged black lines show the rim of the inner and outer calderas. Faults/fissures and eruptive fissures/craters are depicted in blue and yellow, respectively. a) De-trended Bouguer gravity map (mgals) (from Árnason et al., 2007). Gray fault lines define the ESE-WNW transform graben. b) Resistivity map at 1,250 m b.s.l. (from Weisenberger et al., 2015) according to 3D inversion of MT. S-wave shadows mapped by Einarsson (1978) are drawn in purple.

De Zeeuw-van Dalfsen et al. (2006) studied the Krafla volcano by performing micro-gravity measurements in 2002 and 2003 which they compared to previous micro-gravity surveys. They especially highlighted a significant mass decreases at the Krafla caldera, interpreted as a magma drainage. We measured the same gravity stations in summer 2017 and 2018.

4.2 The time-lapse micro-gravity network

A network of 25 stations (see Fig. 8 and Table 2) at the Krafla geothermal area was recorded in summer 2017 and 2018.

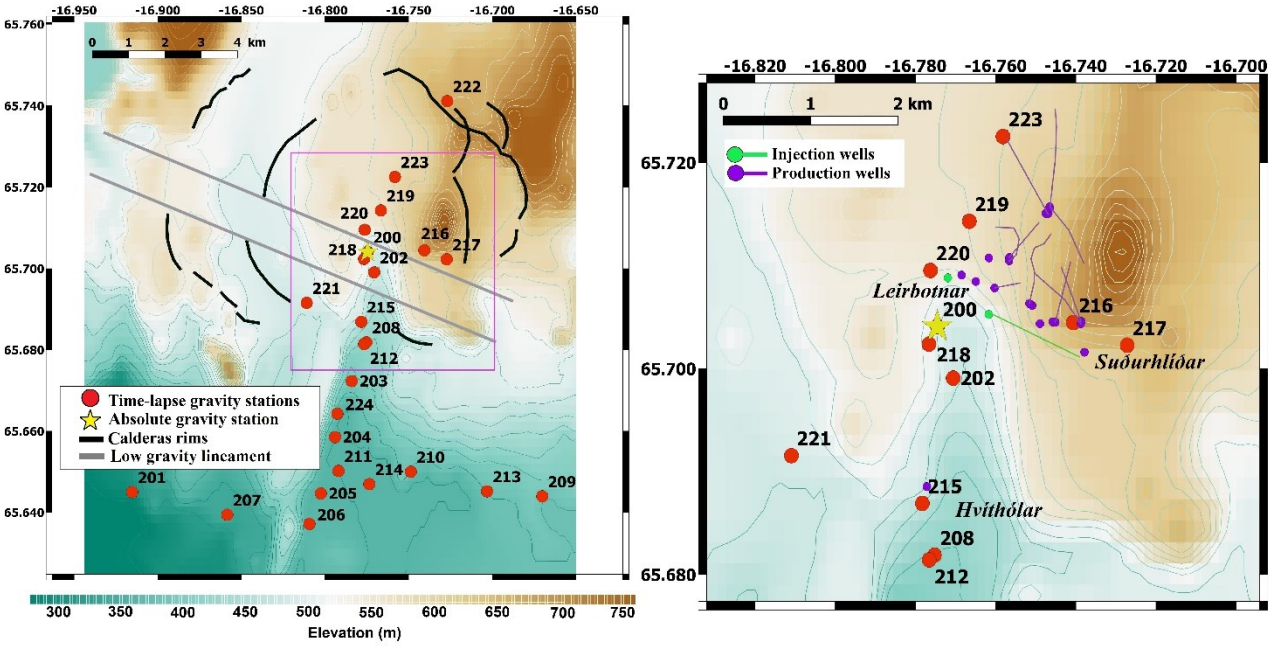

Figure 8: The gravity network of the Krafla geothermal area. Figure to the right is an enlargement of the figure to the left (the pink rectangle). Absolute gravity measurements were performed at the reference station 200 (yellow star). The background topography is from GMTED 2010 with 7.5 arc seconds resolution (www.usgs.gov).

Table 2: Coordinates of the gravity stations at the Krafla geothermal plant.

Stations	Lat.	Lon.	Stations	Lat.	Lon.
200	N 65°42,244'	W 16°46,473'	**213**	N 65°38,712'	W 16°42,185'
201	N 65°38,700'	W 16°54,917'	**214**	N 65°38,817'	W 16°46,410'
202	N 65°41,945'	W 16°46,237'	**215**	N 65°41,215'	W 16°46,697'
203	N 65°40,340'	W 16°47,040'	**216**	N 65°42,269'	W 16°44,438'
204	N 65°39,512'	W 16°47,640'	**217**	N 65°42,137'	W 16°43,633'
205	N 65°38,680'	W 16°48,148'	**218**	N 65°42,144'	W 16°46,598'
206	N 65°38,230'	W 16°48,560'	**219**	N 65°42,858'	W 16°45,995'
207	N 65°38,425'	W 16°51,506'	**220**	N 65°42,572'	W 16°46,575'
208	N 65°40,914'	W 16°46,515'	**221**	N 65°41,494'	W 16°48,657'
209	N 65°38,638'	W 16°40,205'	**222**	N 65°44,469'	W 16°43,615'
210	N 65°39,000'	W 16°44,920'	**223**	N 65°43,352'	W 16°45,492'
211	N 65°39,013'	W 16°47,517'	**224**	N 65°39,858'	W 16°47,558
212	N 65°40,887'	W 16°46,597'			

4.3 The gravity double differences

The gravity double differences recorded in 2018 with respect to 2017 are shown in Figure 9. Similarly as for the Theistareykir network, we only present the values corrected for the gravity change due to vertical displacement deduced from GPS measurements. Sigmundsson et al. describe the deformation study of the Krafla geothermal field in WGC2020 paper n°13174.

The absolute gravimeter measures an increase of 8.9 +/- 2.2 µGal at the reference station. The gravity double differences, corrected for this variation, are all positive. The highest values are close to the two injection areas: We measure an increase of 27 +/- 5 µGal at the station 220 and 20 +/- 4 µGal at the station 216.

4.4 Modelling gravity changes

We explain these highest variations with a simplistic modeling study, by considering only the injected fluid. We calculate the injected sub-surface mass changes M which lead to the measured gravity double differences $Dg_{x-x_0}^{t-t_0}$ using a Mogi sphere (Mogi, 1958) (see equation 3).

$$M = \frac{Dg_{x-x_0}^{t-t_0} * \sqrt{d^2+z^2}^3}{G*z} \quad (3)$$

G is the gravitational constant (6.67×10^{-11} m^3 kg^{-1} s^{-2}). d is the distance of the gravity station to the projection of the injection wells on the surface. z is the depth of the open-hole injection wells (Weisenberger et al., 2015) which corresponds to the center of the Mogi sphere. The result of this first-order modeling is given in Table 3. If we do not take into account the production, the measured gravity double differences can be explained by the injection of 8 MT between summer 2017 and 2018.

Table 3: Calculated mass changes in the Leirbotnar and Suðurhlíðar injection areas.

	Leirbotnar injection area		**Suðurhlíðar injection area**	
z (m) (from Weisenberger et al., 2015)	1199.8		973.3	
Code of the gravity station	220	219	216	217
d (m)	227	675	388	545
The measured gravity double differences $Dg_{x-x_0}^{t-t_0}$ (µGal)	27 +/- 5	11 +/- 4	20 +/- 4	12 +/- 4
The calculated mass changes M (MT) by stations	6.143 +/- 1.138	3.586 +/- 1.304	3.544 +/- 0.709	2.566 +/- 0.855
The estimated mass changes in the area (MT)	~ 5		~ 3	

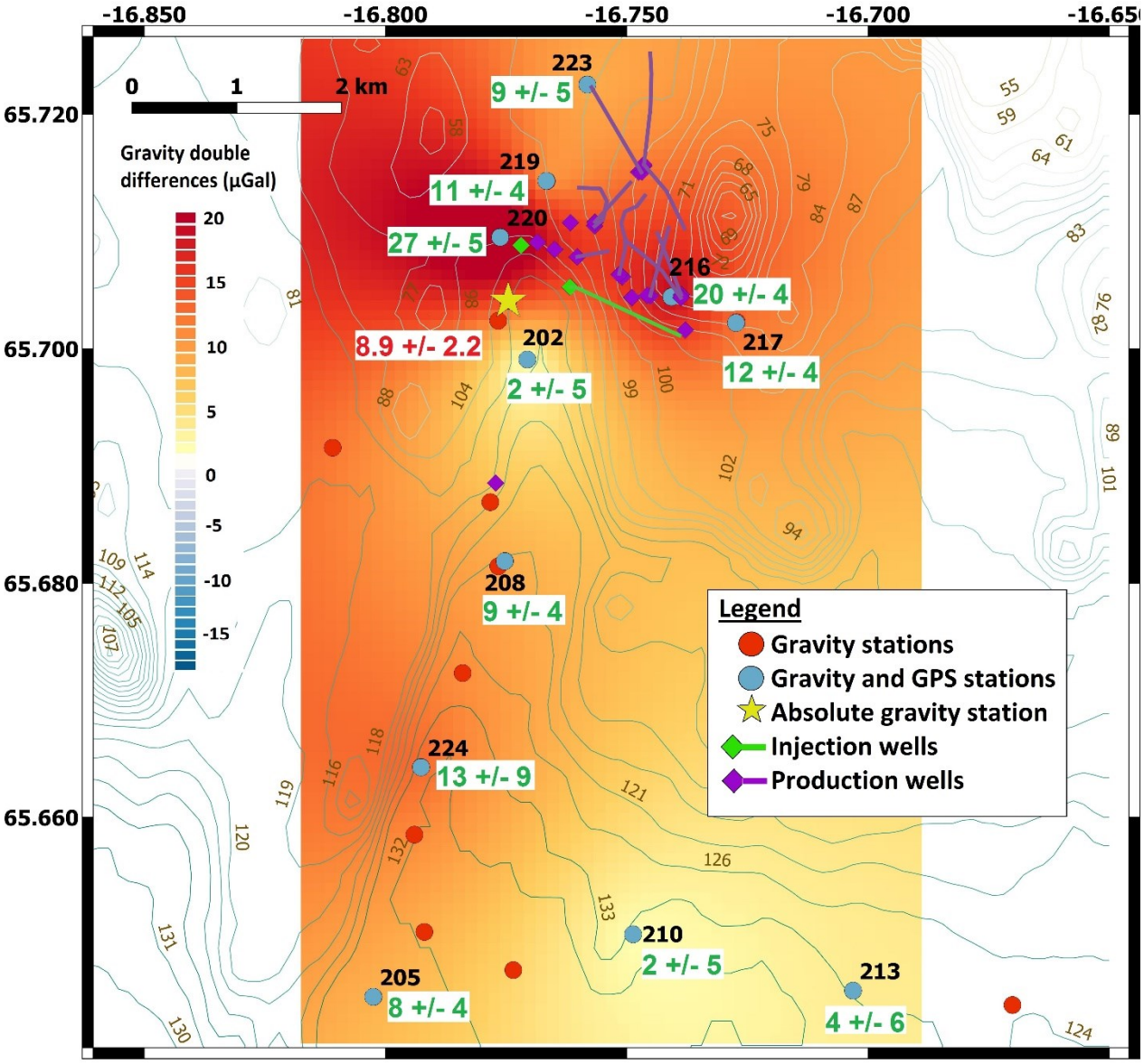

Figure 9: The gravity double differences corrected for the vertical displacement (-3 µGal.cm^{-1}) and the gravity variation of the reference station (yellow star) measured at the Krafla geothermal field in 2018 with respect to 2017. The gravity data have been interpolated using a kriging method. The values and the errors of the absolute (yellow star) and relative measurements are written in red and green, respectively. Black numbers close to the station dots are station number. We distinguish the time-lapse relative stations co-located with GPS sites (blue circle) from those which are not (red circle). The injection and production wells are depicted in green and purple, respectively. We also draw the elevation isolines (m).

4. CONCLUSION

We monitored the gravity variations at the Krafla and Theistareykir geothermal fields in summer 2017 and 2018.

At the Theistareykir site, we notice a gravity decrease in the production area which could be explained by the extraction of 6.5 MT at 1.6 km depth. This gravity decrease is also observed with absolute measurements performed at the west (production) permanent station where a superconducting gravimeter is operating since December 2017: a decrease of 8 µGal is measured between 2018 and 2019 (see WGC2020 paper of Erbas et al., n°13124). The discrepancy in the gravity double differences can be explained by several reasons: 1) The Scintrex CG5 gravimeter is less accurate. 2) The stations are not co-located. 3) We are comparing results for 2017-2018 and 2018-2019 periods. A second gravity decrease is observed in the NW part of the production area. We cannot yet explain this mass change which was already observed before in gravity surveys (2011-2015) by Magnússon (2016) and which is not correlated with the gravity changes induced by the ground water table level change at the well DG-07. Furthermore, no gravity increase is detected near the injection area between 2017 and 2018, which suggests that the reinjected geothermal fluid is drained by faults and moved to another area. To refine our understanding of the Theistareykir geothermal reservoir, we will repeat micro-gravity measurements in summer 2019.

A general increase in gravity is measured at the Krafla geothermal area, with maximum values close to the injection area. The measured gravity double differences can be induced by the injection of 5MT and 3MT at the Leirbotnar and Suðurhlíðar areas, respectively.

Currently, the University of Iceland is working on an InSAR analysis of the two geothermal sites. Once we know the vertical displacements at all the gravity stations, we will be able to refine our interpretation in the light of the new gravity double differences results.

ACKNOWLEDGEMENT

We thank the Landsvirkjun (The National Power Company of Iceland) for the close collaboration, the information exchange and continued support. This work has been carried out under the framework of the LABEX ANR-11-LABX-0050 _G-EAU-THERMIE-PROFONDE and benefits from a State funding managed by the French National Research Agency as part of the Investments Program for the Future.

REFERENCES

Ármannsson, H., Gíslason, G. and Torfason, H.: Surface exploration of the Theistareykir hightemperature geothermal area, Iceland, with special reference to the application of geochemical methods. *Appl. Geochem.* **1**, (1986) , 47-64

Ármannsson, H.: The Theistareykir geothermal system, north east Iceland. Case History. UNU-GTP, KenGen, Kenya (2008)

Árnason, K., Vilhjálmsson, A. M., Björnsdóttir, T.: A study of the Krafla volcano using gravity, micro earthquake and MT data. UNU-GPT, KenGen, Kenya (2007)

Axelsson, G.: Using long case histories to study hydrothermal renewability and sustainable utilization. *GRC Transactions*, **35**, (2011)

De Zeeuw-van Dalfsen, E., Rymer, H., Williams-Jones, G., Sturkell, E., Sigmundsson, F.: Integration of micro-gravity and geodetic data to constrain shallow system mass changes at Krafla Volcano, N Iceland, *Bull Volcanol*, **68**, (2006), 420-431.

Drouin, V., Sigmundsson, F., Verhagen, S., Ofeigsson, B., Spaans, K., Hreinsdottir, S.: *Deformation at Krafla and Bjarnarflag geothermal areas, Northern Volcanic Zone of Iceland, 1993-2015*, Journal of Volcanology and Geothermal Research, **344**, (2017)

Egilson, Þ.: Þeistareykir. Eftirlitsmælingar árið 2018. Report (2019) LV-2019-034 (in icelandic)

Einarsson P.: S-wave shadows in the Krafla caldera in NE-Iceland, evidence for a magma chamber in the crust, *Bull. Volcanol.*, **41**, (1978), 1-9

Hector, B., Hinderer, J.,: PyGrav, a Python-based program for handling and processing relative gravity data. *Comput. Geosci*. **91**, (2016) 90–97

Hinderer, J., Calvo, M., Abdelfettah, Y., Hector, B., Riccardi, U., Ferhat, G., Bernard, J.-D.: Monitoring of a geothermal reservoir by hybrid gravimetry; feasibility study applied to the Soultz-sous-Forêts and Rittershoffen sites in the Rhine graben. *Geotherm. Energy* (2015) 3 -16.

Hinderer, J., Hector, B., Mémin, A., Calvo, M.: Hybrid Gravimetry as a Tool to Monitor Surface and Underground Mass Changes, International Association of Geodesy Symposia. Springer International Publishing Switzerland (2016)

Hjartardóttir, Á., Einarsson, P., Bramham, E., Wright, T.: The Krafla fissure swarm, Iceland, and its formation by rifting events, *Bulletin of Volcanology*, **74** (2012), 2139-2153

Hunt, T., Sugihara, M., Sato, T., Takemura, T.: Measurement and use of the vertical gravity gradient in correcting repeat microgravity measurements for the effects of ground subsidence in geothermal systems. *Geothermics* **31**, (2002) 525–543.

Gíslason, G., Johnsen, G.V., Ármannsson, H., Torfason, H., Árnason, K..: Theistareykir. Surface exploration of the high-temperature geothermal area, Orkustofnun OS-84089/JHD-16 (1984) (In Icelandic).

Guðmundsson, Á., Gautason, B., Axelsson, G., Lacasse, C., Thorgilsson, G., Ármannsson, H., Tulinius, H., Sæmundsson, K., Karlsdóttir, R., Kjaran, S.P., Pálmarsson, S.Ó. and Halldórsdóttir, S.: A conceptual model of the geothermal system at Theistareykir and a volumetric estimate of the geothermal potential.). Iceland GeoSurvey, VGK-Hönnun and Vatnaskil Engineering Office, Report (2008) (In Icelandic)

Kahwa E.: Geophysical exploration of hightemperature geothermal areas using resistivity methods-case study: Theistareykir area, NE Iceland. UNU-GTP, Report 14 (2012).

Karlsdóttir, R., Vilhjálmsson, A.M., Árnason, K., Beyene, A.T.: Theistareykir Geothermal Area, Northern Iceland 3D- Inversion of MT and TEM Data, ISOR-2012/046 Project (2012).

Khodayar, M., Björnsson, S.: Preliminary Fracture Analysis of Þeistareykir Geothermal Field and Surroundings, Northern Rift Zone and Tjörnes Fracture Zone. Report (2013) LV-2013-116

Langella, G., Paoletti, V., DiPippo, R., Amoresano, A., Steinunnardóttir, K., Milano, M.: Krafla geothermal system, northeastern Iceland: Performance assessment of alternative plant configurations, *Geothermics* **69** (2017) 74-92

Mannvit: Theistareykir up to 200 MW geothermal power plant, EIA summary and national planning agency opinion. Report (2015)

Magnússon, I. Þ.: Þyngdarmælingar við Bjarnarflag í ágúst 2011. Íslenskar orkurannsóknir, ÍSOR-2012/076, (2012) (in Icelandic)

Magnússon, I. Þ.: Þyngdarmælingar í Kröflu í ágúst 2013. Íslenskar orkurannsóknir, ÍSOR-2014/007, (2014) (in Icelandic)

Magnússon, I. Þ.: Þyngdarmælingar á Þeistareykjum í júlí til september 2015 og þyngdarkort af Kröflusvæði. Report (2016) LV-2016-090 (in icelandic)

Mkangala, A.: Borehole geology of well ThG-15 at Theistareykir geothermal field NE-Iceland. UNU-GTP Report 18 (2017)

Mogi, K..: Relations between the eruptions of various volcanoes and the deformations of the ground surfaces around them. *Bull. Earthq. Res. Inst*. **36**, (1958) 99–134

Nishijima, J., Umeda, C., Fujimitsu, Y., Takayama, J., Hiraga, N., Higuchi, S.: Repeat Absolute and Relative Gravity Measurements for Geothermal Reservoir Monitoring in the Ogiri Geothermal Field, Southern Kyushu, Japan. *IOP Conf. Series: Earth Environ. Sci.* **42**, (2016) 012004.

Okubo, T., Satomura, M., Furuya, M., Sun, W., Matsumoto, S., Ueki, S., Watanabe, H.: Grand design for the hybrid gravity network around the Mt. Fuji volcano. *International Symponium on Geodesy in Kanazawa*, (2002) Abstract 39–40

Orkustofnun: Energy statistics in Iceland 2017, https://orkustofnun.is/

Portier, N., Hinderer, J., Riccardi, U., Ferhat, G., Calvo, M., Abdelfettah, Y., Heimlich, C., Bernard, J-D.: Hybrid gravimetry monitoring of Soultz-sous-Forêts and Rittershoffen geothermal sites (Alsace, France). *Geothermics.* **76** (2018) 201-219

Saemundsson K.: Jardfraedi Kröflusvaedisins, *Náttúra Mývatns*, ed. Arnthór Gardarsson and Árni Einarsson (1991) (in icelandic)

Saemundsson K.: Geology of the Theistareykir area. ÍSOR – Iceland GeoSurvey, Reykjavík, report ÍSOR-07270 (2007) 24-95 (in Icelandic)

Weisenberger, T. B., Axelsson, G., Arnaldsson, A., Blischke, A., Óskarsson, F., Ármannsson, H., Blanck, H., Helgadóttir, H. M., Berthet, J.-C., Árnason, K., Ágústsson, K., Gylfadóttir, S. S., Guðmundsdóttir, V.: Revision of the Conceptual Model of the Krafla Geothermal System. Report (2015) LV-2015-040

Wolfe, C.J., Bjarnason, I. Th., VanDecar, J.C., Solomon, S.C.: Seismic structure of the Iceland mantle plume, *Nature*, **385**, (1997), 245-247.